

Propagation Characteristics of L_g across the Tibetan Plateau

by D. E. McNamara,* T. J. Owens, and W. R. Walter

Abstract We present the results of a study on the propagation of L_g within the Tibetan Plateau. We analyze over 1200 seismograms for L_g propagation from 185 local and regional earthquakes recorded at distances from 150 to 2000 km, 52 of which are located within the Tibetan Plateau. Although the propagation of L_g has been observed across most of Asia, L_g has not been observed for paths crossing the Tibetan Plateau. We analyze paths that cross the plateau boundaries and paths contained entirely within the Tibetan Plateau. L_g is generated within the Tibetan Plateau and can propagate to epicentral distances of at least 600 km. For events located outside of the Tibetan Plateau, L_g is either absent or severely diminished for paths that cross both the Himalayan and Kunlun ranges, confirming that the margins of the plateau weaken L_g transmission.

Based on the observations from our qualitative analysis, we invert L_g amplitudes for event/station paths that are confined to the Tibetan Plateau to estimate the quality factor, Q . The inversion yields a frequency-dependent Q function:

$$Q(f) = (366 \pm 37)f^{(0.45 \pm 0.06)} \quad (0.5 \leq f \leq 16 \text{ Hz}).$$

Similar observations in other areas indicate that frequency-dependent apparent Q within the Tibetan Plateau is well below that expected for a typical continental interior. Instead, it has a frequency dependence that is characteristic of a tectonically active region.

Introduction

Regional differences in the attenuation of seismic waves have been recognized since it was noticed that the shaking intensity of earthquakes in the western United States decreases faster with epicentral distance than comparable-sized earthquakes in the central and eastern United States (Richter, 1958; Nuttli *et al.*, 1979). With the advent and subsequent abundance of modern instrumentation, amplitude measurements with respect to epicentral distance of fundamental-mode Rayleigh waves and regional phases, such as L_g , have confirmed that attenuation in the western United States is significantly higher than in the eastern United States (Mitchell, 1975, 1981; Frankel *et al.*, 1990). In fact, it has been observed throughout the world that L_g attenuation is higher for regions with active tectonism than for stable continental interiors (Aki, 1980a, 1980b).

L_g is commonly thought to be generated by a superposition of higher-mode surface waves (Oliver and Ewing, 1957; Mitchell, 1995) or multiple reflected shear energy in the crust (Gutenberg, 1955). L_g travels with a group velocity

of about 3.5 km/sec and is prominent on all three components of motion on regional short-period seismograms. In stable continental regions, it is observed at distances as great as 4000 km and has been widely used to estimate earthquake magnitudes and seismic moment for events at regional distances (Nuttli, 1973; Street *et al.*, 1975; Herrmann and Kijko, 1983). L_g has been successfully modeled as a higher-mode surface wave (Ewing *et al.*, 1957; Knopoff *et al.*, 1973), and the group velocity of L_g implies that it propagates as multiple reflected shear waves trapped within the crust (Press and Ewing, 1952; Herrin and Richmond, 1960; Bouchon, 1982). It is commonly observed that lateral heterogeneity plays a significant role in shaping the characteristics of the L_g signal (Ruzaikin *et al.*, 1977; Kennett *et al.*, 1985). Consequently, L_g carries information about the average crustal shear-wave velocity and apparent attenuation along its path and is sensitive to varying tectonic environments.

The observation of L_g is often used to infer the existence of continental crust because L_g does not propagate across oceanic crust; it can be shown that L_g quickly loses energy in the thin wave guide provided by oceanic crust (Kennett, 1986). Also, L_g propagation is affected by variations of the crustal wave guide along its path. For example, Aki (1980a)

* Present address: Lawrence Livermore National Laboratory L-202, Livermore, California 94550. E-mail: dmcnamara@llnl.gov.

proposed that scattering of Lg energy from fractures within the crust, in tectonically active regions, is a major cause of strong Lg attenuation. A disruption of Lg propagation can also be caused by the lack of a continuous wave guide. For example, strong attenuation of Lg can occur in areas where significant crustal thickness variations exist (Gregersen, 1984; Ruzaikin *et al.*, 1977; Rodgers *et al.*, 1995; Cao and Muirhead, 1993; Campillo, 1987; Kennett, 1986).

Lg has been observed across much of Asia; however, Lg has not been observed for paths crossing through the Tibetan Plateau (Ruzaikin *et al.*, 1977; Ni and Barazangi, 1983; Bath, 1954; Pec, 1962; Saha, 1961). This effect has been attributed to either scattering due to a change in the crustal thickness and/or structural discontinuities at the boundaries of the plateau or to an unusual velocity structure or high attenuation within the plateau (Ruzaikin *et al.*, 1977). Previous studies were limited since they had to rely on stations outside of the Tibetan Plateau and could only observe Lg for paths that cross the boundaries of the plateau. Consequently, they were unable to distinguish between the effects that the interior of the plateau versus its boundaries may have had on Lg amplitudes.

In this article, we study the nature of Lg propagation and attenuation within the Tibetan Plateau. First, we qualitatively analyze Lg attenuation and blockage by visually inspecting Lg amplitudes for paths crossing through the Tibetan Plateau and surrounding regions. Second, we invert Lg amplitudes, from paths restricted to the Tibetan Plateau, for frequency-dependent attenuation. Frequency-dependent Q can be modeled as

$$Q(f) = Q_0 f^\eta, \quad (1)$$

where Q_0 is the quality factor, Q , at a frequency, f , of 1 Hz and the exponent η describes the frequency dependence of Q . $Q(f)$ values vary considerably depending on the tectonic style of the region of Lg propagation. For example, Chavez and Priestley (1986) found Lg $Q(f) = 214f^{0.54}$ within the tectonically active basin and range province of North America while Atkinson and Mereu (1992) showed that frequency-dependent Q in tectonically stable southeastern Canada is as high as $Q(f) = 670f^{0.33}$. In general, Q_0 is small and η is large for tectonically active regions relative to more stable continental interiors.

Data used in this study were digitally recorded using 3-component, broadband sensors at 11 sites within the central portion of the Tibetan Plateau (Fig. 1, Table 1). At 10 of the stations, data were collected in an event-triggered mode at 40 samples per second (sps). LHAS operated in a continuously recording mode at 5 sps (Fig. 1) (Owens *et al.*, 1993a, 1993b). Instrumentation for this experiment consisted of 10 Streckeisen STS-2 sensors and one Guralp CMG-3ESP at the TUNL station (Fig. 1). The STS-2 and Guralp are both active feedback seismometers. The STS-2 has flat velocity response between 1/120 and 50 Hz, and the CMG-3ESP has corner frequencies of 1/30 and 30 Hz (see Owens *et al.*,

1993a). Over 1200 seismograms from 185 regional events were examined for the existence of Lg . Of these, 52 events provided paths that travel entirely within the Tibetan Plateau. Event locations are determined from the USGS PDE's and are shown in Figure 1.

Lg Propagation within the Tibetan Plateau and Surrounding Regions

Our qualitative analysis of Lg is similar to the method applied by Ruzaikin *et al.* (1977) and to the mapping of Sn propagation within the Tibetan Plateau (McNamara *et al.*, 1995; Ni and Barazangi, 1983). The procedure consists of two parts. First, we merely note if Lg is present, absent, or weak on both the tangential and radial component high-pass filtered (>0.5 Hz) event record sections at the time appropriate for a wave traveling at a typical continental Lg velocity (3.1 to 3.6 km/sec). A weak Lg arrival is defined as one with an amplitude less than half that of the vertical-component P coda. Second, to better constrain the spatial distribution of Lg propagation characteristics, we map event/station paths, coded to represent our amplitude observations. We were able to observe Lg within a range of path lengths from several hundred to several thousand kilometers. We focused on events with epicentral distances greater than 150 km for two reasons. First, in many cases with short epicentral distances, it was difficult to determine the presence of Lg because of interference with that of the higher amplitude S arrivals. Second, by using events with distances greater than 150 km, we can assume a constant geometrical spreading (Street *et al.*, 1975; Atkinson and Mereu, 1992; Burger *et al.*, 1987).

The most significant new observations from our data set is that Lg propagates within the Tibetan Plateau and that both the northern and southern boundaries of the plateau cause inefficient Lg propagation. We have observed strong Lg at all plateau stations from events with epicenters also located within the plateau. Previous studies have had few recording stations on the plateau and thus limited opportunity to observe Lg that did not cross the margins of the Tibetan Plateau. Though Lg is generated on the plateau, for our data set ($mb = 3.7$ to 5.5), we find that energy is quickly attenuated for event/station paths within the plateau that are greater than about 600 to 700 km. Events to the north do not have observable Lg energy at recording stations >100 km into the plateau, suggesting that the northern boundary diminishes Lg amplitudes. We do, however, observe Lg at our stations near the northern edge of the plateau (TUNL and MAQI) for long paths (>700 km) from the same events to the north of the plateau, suggesting that the Tarim and Qaidam Basins allow more efficient propagation of Lg than the Tibetan Plateau. We also confirm previous observations that the southern boundary of the Tibetan Plateau blocks Lg propagation (Ruzaikin *et al.*, 1977; Ni and Barazangi, 1983).

Figures 2a and 2b are maps showing selected paths to demonstrate the spatial distribution of Lg propagation with-

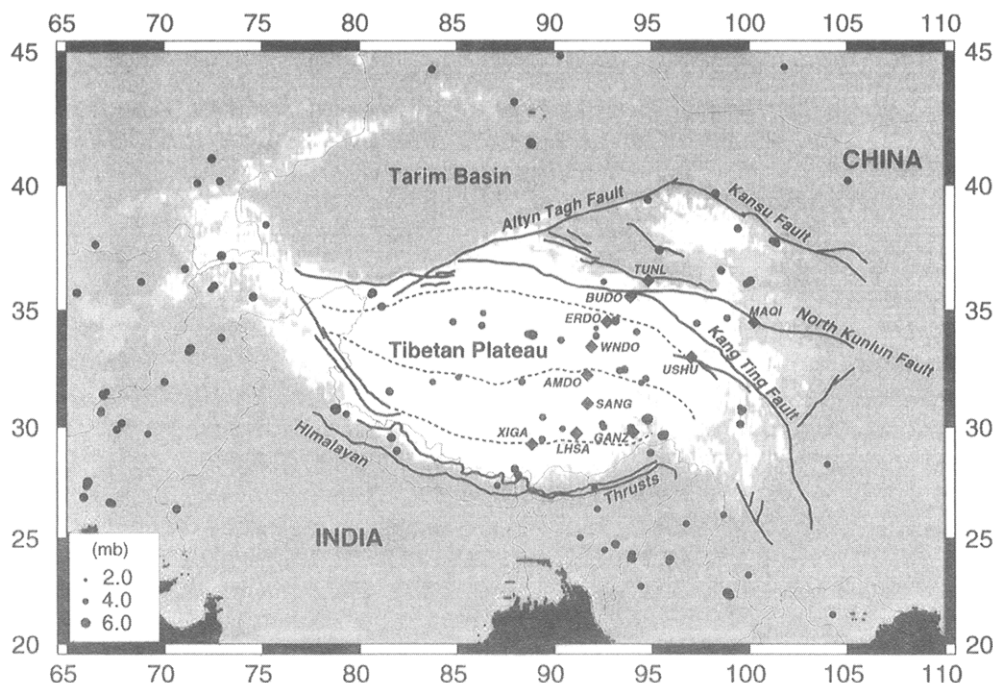


Figure 1. Tibetan Plateau experiment base map showing recording stations (gray diamonds) and the distribution of regional events (solid circles) used to map *Lg* propagation. Regional structural trends are taken from Dewey *et al.* (1988). Solid lines show major faults, and dashed lines indicate suture zones that bound tectonic terranes of the plateau. Elevation is shown shaded with 1000-m contour intervals. The area in white is above 4000-m elevation and is considered the boundary of the Tibetan Plateau for our study.

Table 1
Tibetan Plateau Seismic Experiment (Station Locations)

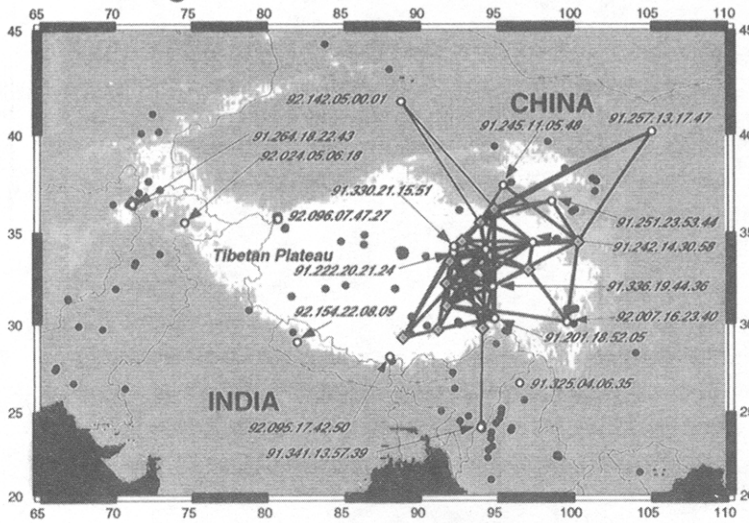
Station	Latitude (°N)	Longitude (°E)	Elevation (m)
AMDO	32.247	91.688	4712
BUDO	35.529	93.910	4660
ERDO	34.520	92.707	4623
GANZ	29.767	94.050	3150
LHASA	29.702	91.128	3700
SANG	31.024	91.700	4740
TUNL	36.199	94.815	3133
WNDO	33.448	91.904	4865
XIGA	29.234	88.851	3865
MAQI	34.478	100.249	3823
USHU	33.011	97.015	3727

out obscuring the important points with our abundance of data. Figure 2a shows that a majority of paths where *Lg* is observed are associated with events within the plateau. Most of these paths are short and restricted to the eastern plateau. At stations within the plateau, a small number of paths with observed *Lg* energy are from events outside of the plateau. In nearly all cases, paths crossing the Kunlun and Himalaya ranges have little *Lg* energy. However, in some cases, for events outside of the plateau, *Lg* is observed at stations toward the edges of the plateau. More specifically, two stations

approximately 100 km from the 4000-m contour (BUDO and GANZ) record *Lg* from events outside of the plateau (Fig. 2a). This suggests either a transition zone of *Lg* attenuation or that *Lg* is scattered and can propagate a short distance before it is entirely “attenuated” or “blocked.” Figure 2b shows that a majority of regional paths that cross the Tibetan Plateau do not contain significant *Lg* arrivals. These are either long paths within the Tibetan Plateau or paths crossing its boundaries.

Record sections are shown in Figures 3 and 4 to demonstrate *Lg* propagation for some paths shown in Figure 2. Event 91.222.20.21.24 is an example of an event within the Tibetan Plateau, and sample seismograms are shown in Figure 3. This event was located between ERDO and WNDO in the array, within the central portion of the plateau (Fig. 2). For events within the plateau, recorded at stations within the plateau, *Lg* energy is observable out to distances of 600 to 700 km. Energy and frequency content steadily decrease with epicentral distance. By examining paths from many event locations, we find little correlation with *Lg* amplitude decay and internal plateau structure, suggesting that there is no dependence on azimuth. Instead, amplitude decay appears to be primarily related to distance traveled within the plateau, suggesting that intrinsic *Q* is the dominant attenuation mechanism for these paths. Also, the previously identified zone of inefficient *S_n* propagation in the northern pla-

A: Paths with L_g



B: Paths without L_g

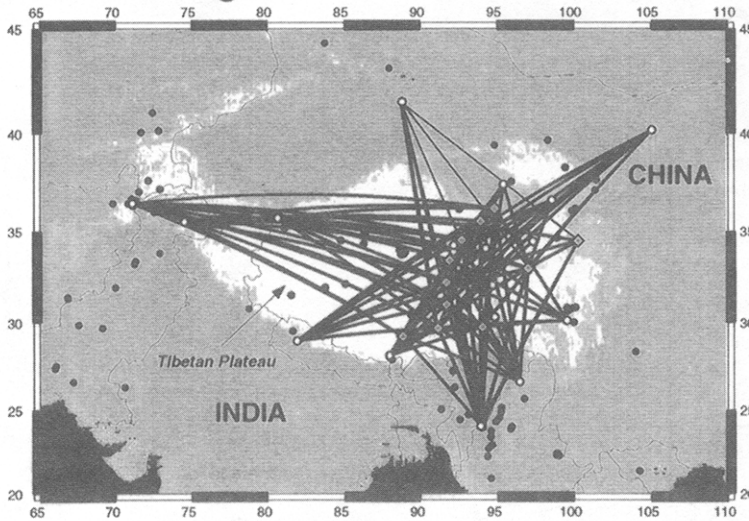


Figure 2. L_g propagation characteristics across the plateau. Events selected to demonstrate L_g characteristics are shown with an open circle. Event identifiers are the same as in Table 2. (a) Map of paths where L_g is observed. (b) Map of paths where L_g is not observed.

teau (Ni and Barazangi, 1983; McNamara *et al.*, 1995) does not appear to affect L_g amplitudes. This would suggest that while mantle properties vary across the Tibetan Plateau, attenuation of L_g in the crust is laterally uniform.

For paths that cross into the Tibetan Plateau from outside, there is little observable L_g energy. We show an example of how the northern boundary of the plateau blocks L_g transmission using event 91.257.13.17.47 (Fig. 4). This is an event from northeast of the array and shows L_g energy at stations at the northern end of the array (TUNL, MAQI, BUDO, and USHU). Since the magnitude of the earthquake ($m_b = 5.1$) is similar to events examined within the plateau, the presence of energy at TUNL and MAQI suggests that L_g will propagate at long distances (>700 km) outside of the plateau. L_g amplitude is significantly decreased as paths propagate into the plateau. The weak presence of energy at stations USHU and ERDO for the same event demonstrates that the boundary does not abruptly block L_g transmission.

Instead, energy diminishes across about 200 km of the plateau path. These observations are unambiguous since the stations within the plateau have similar azimuths for these events, and thus, the absence of L_g can be attributed to the margins of the plateau rather than to the source radiation patterns.

The southern boundary of the Tibetan Plateau also has a dramatic effect on L_g and has been demonstrated in previous studies (Ruzaiкин *et al.*, 1977; Ni and Barazangi, 1983). For events south of the Tibetan Plateau, the amplitude of L_g quickly dies out at stations progressively northward into the plateau. Events 91.341.13.57.39, 91.325.04.06.35, and 92.154.22.08.09 are located southwest of the array to the south of the Tibetan Plateau and the Himalayan boundary thrust (Fig. 2). Both show practically no L_g energy at our recording stations, with the exception of some southern stations (GANZ and XIGA). In these cases, L_g amplitudes are quite small, and energy quickly decays progressively to the

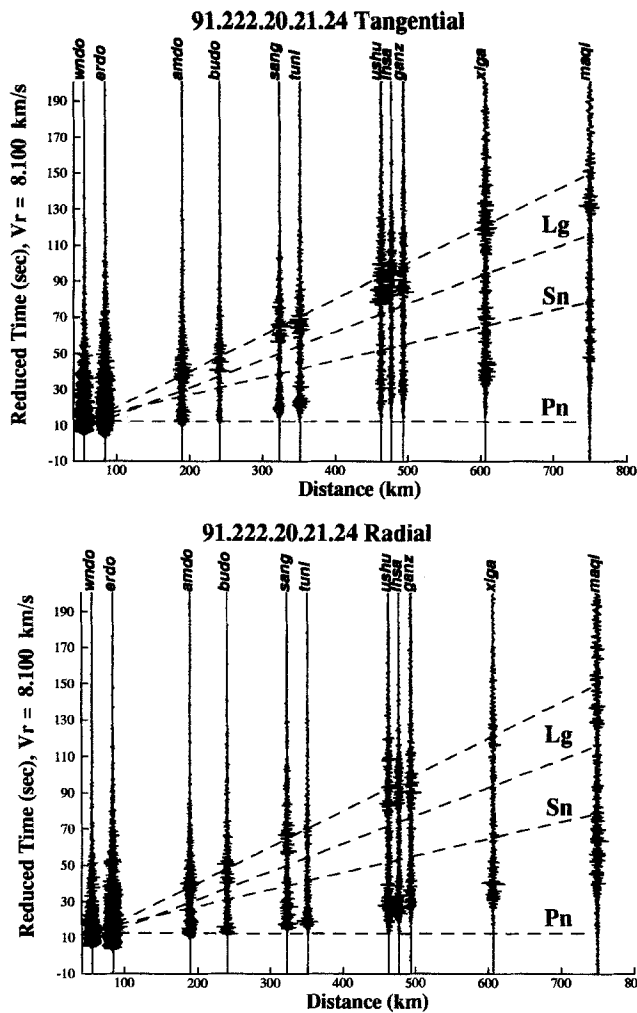


Figure 3. Central plateau event record section (91.222.20.21.24, $m_b = 5.4$). Both the tangential (left) and radial (right) components of motion are shown high-pass filtered (>0.5 Hz) with the exception of LHASA. Data at the LHASA station was obtained at a slower sampling rate of 5 samples/sec. Consequently, seismograms are shown band-pass filtered with corner frequencies of 0.5 and 2.0 Hz. Dashed lines show the predicted arrival times of *Pn* (8.1 km/sec), *Sn* (4.6 km/sec), and *Lg* (3.6 to 3.1 km/sec) (McNamara *et al.*, 1995). The recording station is shown at the end of each record section trace.

north. Ni and Barazangi (1983) suggested that the Indus-Zangbo suture zone rather than the Himalaya is the boundary that blocks *Lg* energy from entering the plateau. Due to limited ray coverage, we are not able to resolve this distinction.

We have shown that *Lg* is generated within the plateau but does not propagate efficiently to distances greater than about 600 to 700 km for our data set ($m_b < 5.5$). This implies a high attenuation for paths within the plateau, as predicted by Molnar and Oliver (1969) and Ruzaiкин *et al.* (1977). We have also shown that *Lg* energy is strongly attenuated for all paths that cross the margins of the plateau defined by the Himalaya and Kunlun mountain ranges to the

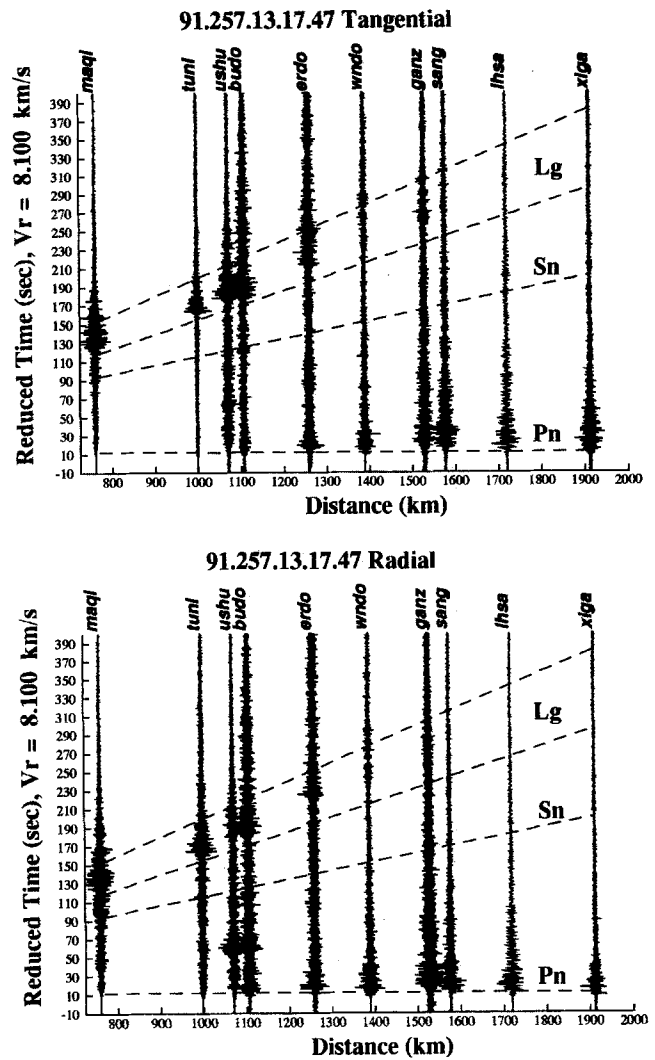


Figure 4. Regional event, from northeast of the plateau (91.257.13.15.47, $m_b = 5.1$). Display parameters are the same as Figure 3.

south and north, respectively. While attenuation for *Lg* paths within the plateau is high, the dominant effect contributing to the demise of *Lg* for paths entering the plateau is at its margins. High attenuation within the plateau is, however, a significant contributing factor. In the next section, we present our inversion of observed *Lg* amplitudes for frequency-dependent apparent *Q* to quantify Tibetan Plateau crustal attenuation.

Measurement of Frequency-Dependent *Lg* *Q* within the Tibetan Plateau

Q Inversion Method. We have shown that *Lg* is generated within the Tibetan Plateau and that the amplitude of *Lg* decreases quickly with increasing epicentral distance within the plateau. These observations imply that attenuation is high within the plateau. In order to quantify the attenuation, we examined the amplitudes of *Lg* arrivals from events

within the Tibetan Plateau to estimate apparent Q (Fig. 1). The quality factor, Q , provides attenuation information about the medium in which Lg propagates when compared with other regions throughout the world.

The observed amplitude of Lg can be modeled as

$$A(f, D) = \frac{1}{D^{2\lambda}} R(f)S(f)e^{-\pi f D/\nu Q(f)}, \quad (2)$$

where D is the hypocentral distance, R is a receiver term that denotes site effects, S is the term that represents the individual earthquake source excitation, f is the median frequency of the observed wave, ν is the group velocity for Lg (3.5 km/sec), λ is the exponent of the geometric spreading within the medium, and $Q(f)$ is the quality factor of Lg propagation within the crust.

Rewriting and taking the natural log of both sides of (2) yields

$$\ln[A(f, D)D^\lambda] = \ln[R(f)] + \ln[S(f)] - \frac{\pi f D}{\nu Q(f)}. \quad (3)$$

When the left-hand side of (3) is plotted against distance, (3) describes a line where the R and S terms control the intercept and the Q term controls the slope.

Since the response of our instruments is well known (Owens *et al.*, 1993a), we directly solve for the source and receiver terms as well as the regional $Q(f)$ by inverting instrument-corrected and geometrical-spreading-corrected Lg amplitudes from many different events recorded at the stations within our array (Benz *et al.*, 1994). Using our data set of many source-receiver pairs, a system of linear equations can be set up based on equation (3). The system of equations can be expressed as

$$\mathbf{Ax} = \mathbf{t}, \quad (4)$$

where \mathbf{A} is a matrix made up of the parameter coefficients of (3). It contains mostly ones and zeros, with one column listing a portion of the last term of (3) ($-\pi f D/\nu$). The vector \mathbf{x} contains the unknowns S for each event, R for each station, and the regional Q term. The \mathbf{t} vector contains the left-hand side of equation (3). By fixing f , we know A , D , and ν for each source-receiver pair. We then solve for S of each event, R of each station, and Q using a singular-value decomposition inversion technique (e.g., Menke, 1990). By performing the inversion over several frequency bands, we obtain a measure of frequency-dependent $Q(f)$. Since we do not consider the effects of scattering or radiation pattern, and assume a reasonable geometric spreading, our measure is apparent rather than intrinsic Q . Radiation effects should be minimal since Lg consists of a large number of reflected rays that distribute energy across all three components of motion.

Before we can obtain a measure of regional Lg $Q(f)$, several assumptions must be considered. Generally, the Lg

wave train is comprised of the high-frequency energy (>0.5 Hz) that propagates with a group velocity ranging from 3.6 to 2.8 km/sec at regional distances (Street *et al.*, 1975; Nuttli, 1973; Press and Ewing, 1952; Atkinson and Mereu, 1992; Campillo, 1990). Based on our qualitative analysis of Tibetan Plateau data, we observe that the main Lg energy arrives within the group velocity window 3.6 to 3.1 km/sec. Since Lg is not dispersive, we assume the generally accepted frequency-independent group velocity of 3.5 km/sec and find that the inversion is relatively insensitive to propagation velocity. Inversions using the mid-window group velocity ($\nu = 3.4$ km/sec) did not significantly alter resultant Q values.

The selection of the geometric spreading coefficient, γ , is critical since it is sensitive to the velocity structure of the crust (Banda *et al.*, 1982) and has been shown to trade off with resultant values of Q (Atkinson and Mereu, 1992; Campillo *et al.*, 1984). Lg Q measurements in the frequency domain have shown that for local sources (<130 km), γ is approximately 1.0. At distances beyond 130 km, Lg amplitude decays less steeply (Atkinson and Mereu, 1992). In this case, a geometric spreading coefficient of $\gamma = 0.5$ is used. This is the conventional model for regional surface waves (Street *et al.*, 1975) and holds true for other regions (Frankel *et al.*, 1990). Our approach uses Lg amplitude measurements in the time domain, so we must assume a geometric attenuation that corrects for the spectral density per time unit. Since signal duration increases with distance, attenuation is greater in the time domain. Thus, a larger geometric spreading coefficient, $\gamma = 0.83$, is generally assumed in the time domain relative to the frequency domain (Campillo *et al.*, 1984; Campillo, 1990; Nuttli, 1973). Underestimating γ leads to an underestimation of Q_0 and an overestimation of η . For this reason, the higher value, $\gamma = 0.83$, assumed for our time domain amplitudes will result in a more accurate estimate of Lg Q .

Data Selection and Preparation. For our analysis, we restrict the data to events with paths confined to the Tibetan Plateau. Since we have shown that the boundaries of the plateau diminish Lg amplitudes, this step will eliminate paths with weak Lg that may contaminate the plateau measure of Q . Figure 5 is an example of the Lg phases used in the inversion. We first computed the instrument-corrected, displacement seismogram of the bandpass-filtered tangential component of motion. Selection of the tangential component is based on the observation, from the previous section, that energy is greater and more consistent across more passbands on the tangential than on the vertical or radial components of motion. As a test, we ran the inversion on amplitudes measured from the vertical component and found that resulting Q values were within one standard deviation of the results acquired with tangential component amplitudes. This supports our assumption that Lg energy is distributed across all components of motion and that decay of amplitude with increasing distance is consistent across all components of

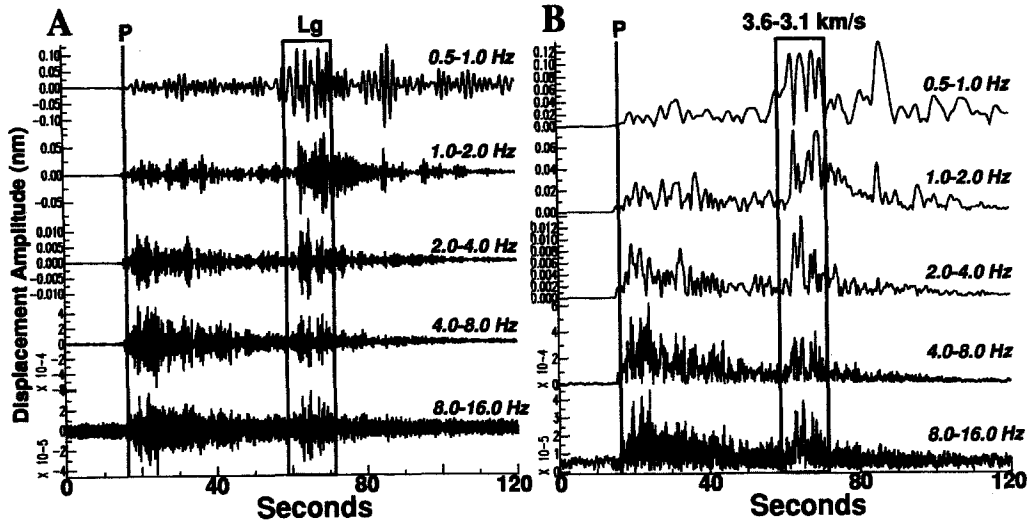


Figure 5. An example of *Lg* amplitudes measured in five passbands used in the inversion. Event 92.143.05.46.46 ($m_b = 4.6$) from the southeastern Tibetan Plateau, recorded at USHU, at a distance of 356 km. Traces are scaled individually to show the relative amplitudes of the *P* and *Lg* phases. (a) Tangential component of the instrument-corrected displacement seismograms for passbands used in the inversion. (b) Envelopes of seismograms shown in (a). *Lg* amplitude was taken as the maximum amplitude within the window between 3.6 and 3.1 km/sec.

motion. We did find, however, that at high frequencies (>6 Hz), we were unable to obtain enough high signal-to-noise *Lg* phases on the vertical component to compute Q . In general, signal to noise was best on the tangential component for all passbands examined.

Each filtered seismogram was then smoothed about the mean of a 10-sample moving window. Next, we determined the seismogram envelope $E(t)$ from

$$E(t) = [A(t)^2 + H(t)^2]^{0.5}, \quad (5)$$

where $A(t)$ is the smoothed, bandpassed time series and $H(t)$ is its Hilbert transform. We used the maximum amplitude within a window bounded by velocities of 3.6 to 3.1 km/sec. Examples of *Lg* amplitudes for one event, filtered in 1 octave passbands, are shown in Figure 5.

Prior to the inversion, *Lg* signal to noise was examined to eliminate random errors in the amplitude measurements. Specifically, we only wish to include amplitudes in the inversion where *Lg* is present. For the signal-to-noise analysis, shown in Figure 6, the *Lg* signal was taken as the average amplitude within the *Lg* group velocity window, and the noise was measured as the average amplitude for an additional 50 sec behind the *Lg* window. Figure 6 shows the signal-to-noise ratio versus epicentral distance for *Lg* amplitudes in the 2- to 4-Hz band, for paths from 52 events within the Tibetan Plateau. The many cases with signal-to-noise ratios much greater than 10 are not plotted so as to demonstrate the differences at low signal-to-noise ratios. For the inversion, we selected only *Lg* phases with a signal-to-noise ratio of 2 or greater. In Figure 6, we see that this

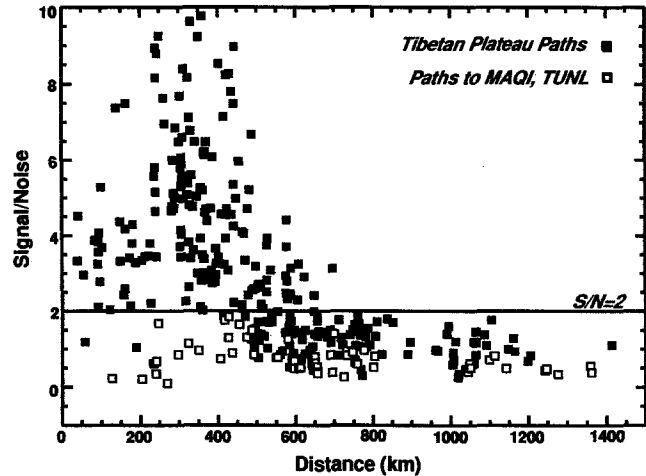


Figure 6. *Lg* signal to noise versus epicentral distance in the 2- to 4-Hz band, for 52 events located within the Tibetan Plateau. Closed squares show the average amplitude between 3.6 and 3.1 km/sec divided by the average amplitude for 50 sec beyond the *Lg* window for paths confined to the Tibetan Plateau. Open squares show signal to noise for paths that cross the northern boundary of the plateau to TUNL and MAQI. Paths with signal to noise of 2 or greater were used in the inversion for Q .

criteria eliminates all paths within the plateau greater than about 700 km as well as all paths crossing the northern boundary of the plateau to stations TUNL and MAQI. This observation is consistent with our qualitative amplitude observations discussed in the previous section. We also required that each station record at least two events and that

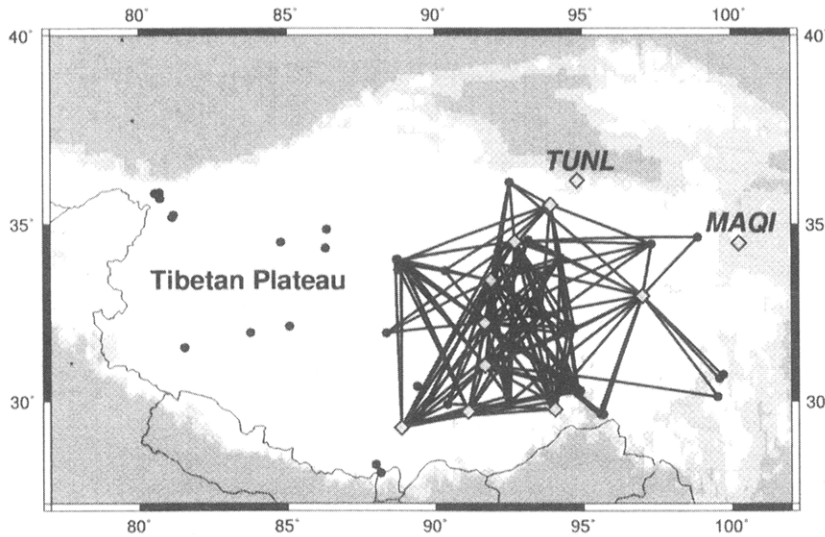


Figure 7. Paths with L_g signal to noise equal to or greater than 2 in the 2- to 4-Hz frequency band.

each event was recorded by at least two stations. In the 2- to 4-Hz band, this leaves 106 observations from 20 events recorded at eight different stations (Fig. 7). Ray-path coverage is similar for the additional frequency bands and is generally restricted to the eastern portion of the plateau. As demonstrated in the qualitative section presented earlier, longer paths from western plateau events do not contain measurable L_g energy. Therefore, our final $Q(f)$ is representative of only the eastern portion of the Tibetan Plateau due to our station coverage and small magnitudes of the events in our data set.

Inversion Results. By repeating the inversion over a range of five different fixed frequency bands, we obtain a measure of frequency-dependent $Q(f)$. The inversion was performed over five octaves with center frequencies of 0.75, 1.5, 3, 6, and 12 Hz. Figure 8 shows L_g amplitude data with the source and receiver contributions removed. Straight lines represent the best-fitting Q for the particular frequency band. As is often observed, Q increases with increasing frequency; however, our measured Q for the Tibetan Plateau is low relative to other continental regions (Benz *et al.*, 1994). As shown in equation (1), Q can be expressed as a function of frequency. Taking the log of both sides of equation (1) yields

$$\log[Q(f)] = \log[Q_0] + \eta \log[f], \quad (6)$$

which is an equation for a straight line where $\log[Q_0]$ is the intercept and η controls the slope. We use the standard deviation of the resultant Q fit for each passband as a weight and determine the best-fit line in the range of passbands (0.5 to 16 Hz) for a measure of $Q(f)$. A weighted least-squares fit to the plateau data is shown in Figure 9 and gives

$$Q(f) = (366 \pm 37.0)f^{(0.45 \pm 0.06)} \quad (0.5 \leq f \leq 16 \text{ Hz}).$$

As observed in Figure 9, our measured $Q(f)$ is low and more

consistent with values obtained from tectonically active regions.

Discussion

The lack of L_g energy for paths crossing the Tibetan Plateau has been attributed to either a change in the crustal wave guide at the boundaries of the plateau or to complications to the wave guide within the interior of the plateau itself. The crust within the Tibetan Plateau is thicker than surrounding regions, such as the Indian Shield to the south and the Tarim Basin to the north (Molnar, 1988; Christensen and Mooney, 1995). L_g amplitude can decrease as it encounters the crustal thickness transitions at the margins of the Tibetan Plateau. Also, the complicated structures that bound the plateau, such as the southern Himalayan boundary thrust and the northern Kunlun fault, could cause scattering of L_g energy, significantly decreasing its observable amplitude. Causes of L_g attenuation due exclusively to the interior of the plateau could be attributed to intrinsic attenuation; unusual velocity structure due to the anomalously thick plateau crust; or scattering caused by faults, fractures, and interstitial fluids within the crust (Aki, 1980a; Ruzaiкин *et al.*, 1977; Gregersen, 1984; Frankel *et al.*, 1990; Mitchell, 1995). All are likely candidates to explain the observed L_g amplitude decrease for paths crossing the Tibetan Plateau. In the following sections, we explore these ideas in more detail.

L_g Attenuation at the Boundaries of the Tibetan Plateau. Previous studies have reported that L_g is not observed for paths crossing the Tibetan Plateau (Ruzaiкин *et al.*, 1977; Ni and Barazangi, 1983). Since L_g is a crustal wave train, its absence can be caused by significant changes and/or anomalies in the crustal wave guide. Ruzaiкин *et al.* (1977) have speculated that L_g is disrupted at the margins of the plateau by a change in crustal thickness or by the absence of the crustal “granitic layer.” Alternately, they suggest that L_g

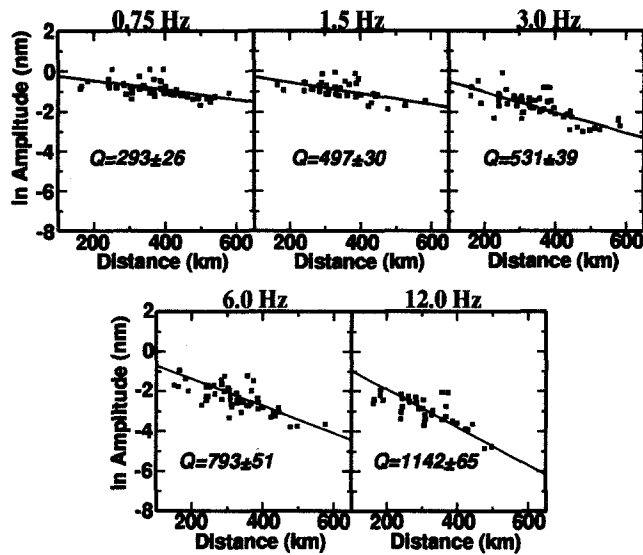


Figure 8. Best-fit Q determined from the inversion over several passbands.

does not efficiently propagate within the plateau at all due to extremely high intrinsic attenuation within the plateau itself. Our results suggest that both mechanisms may contribute to the absence of L_g ; however, the boundaries of the plateau have the most dominant effect. We have shown that L_g is strongly attenuated for paths crossing the margins of the plateau. This indicates that not only the southern boundary, defined by the Himalaya, but the northern Kunlun front is equally efficient at blocking the propagation of L_g . Due to the lack of seismicity to the east of the plateau, in China, we were not able to examine many paths crossing the eastern boundary of the plateau. We have shown that L_g energy can be observed at stations near these boundaries, but it quickly decreases at stations farther within the plateau. This observation suggests that the signal is scattered rather than abruptly removed. If the crustal “granitic” layer, in which L_g propagates, were completely absent within the Tibetan Plateau, then we would expect no L_g within the plateau. Since we have shown that L_g does propagate within the plateau, a variation in crustal thickness across the boundaries rather than a complete removal of the crustal wave guide, as previously suggested, is a more likely interpretation of our observations. Also, Mitchell (1995) suggests that the disruption of L_g propagation could be due to scattering along crustal cracks and faults, or an increased attenuation due to interstitial fluids could significantly diminish L_g amplitudes. This effect could be present with the complicated structures at the boundaries of the plateau.

To generate realistic L_g arrivals and effectively analyze propagation characteristics due to lateral heterogeneities, relatively sophisticated techniques requiring multi-dimensional models are required. Several such attempts have successfully shown that L_g transmission is severely effected by crustal pinching, such as transitions from continental to oceanic crust with an overlying water column and, to a lesser extent,

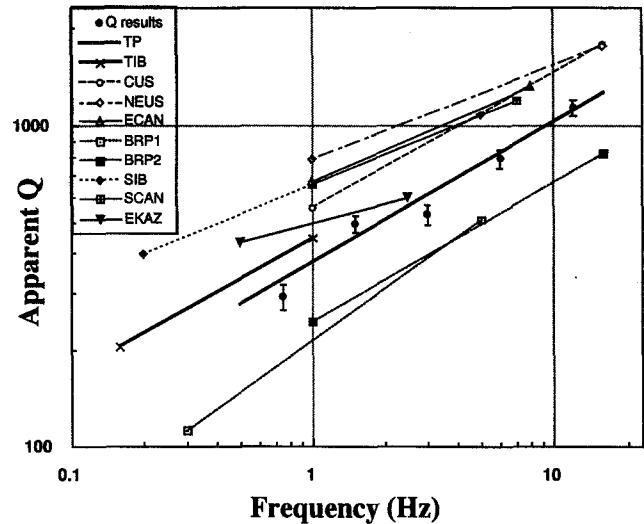


Figure 9. The weighted least-squares $Q(f)$ fit (TP, solid line) to our data (solid circles). Also shown are several other regions for comparison, including the northeastern United States (NEUS), central United States (CUS), basin and range province of North America (BRP1) [Benz *et al.*, 1994, BRP2, Chavez and Priestley (1986)], Russian explosion recorded at stations in Siberia (SIB) (Xie, 1993), eastern Canada (ECAN) (Atkinson and Mereu, 1992), eastern Kazakhstan (EKAZ) (Serenio, 1990), Scandinavia (SCAN) (Serenio *et al.*, 1988), and a previously determined value for the Tibetan Plateau (TIB) at longer periods (Shih *et al.*, 1994).

topography on the Moho or thickening of the crust (Kennett, 1986; Cao and Muirhead, 1993; Campillo, 1990). Few attempts have been made to model the type of scenario that exists at the margins of the Tibetan Plateau. To fully understand the inefficient propagation of L_g in this region, models must be able to distinguish between high attenuation due to intrinsic rock and fluid properties from the effect of waveguide thickness variations.

Lg Attenuation within the Tibetan Plateau. L_g is clearly generated within the Tibetan Plateau; however, for our data set, amplitudes are significantly diminished after traveling several hundred kilometers within the plateau. We have not observed any correlation between propagation direction or path location with the presence or absence of L_g within the plateau. This suggests that while the crustal wave guide is homogeneous enough to allow L_g to propagate, attenuation in the crust is sufficient to rapidly diminish the signal amplitude. We suggest that several geologic factors may contribute to apparent attenuation within the crust and the corresponding inefficient propagation of L_g . First is scattering within the laterally complex crust along fractures and faults bounding the numerous tectonic terranes that make up the plateau. Second, in regions that have undergone recent crustal deformation and tectonic activity, interstitial fluids may be present that enhance attenuation. The fluids could

be the result of melt and metamorphism in the crust due to elevated temperatures from internal deformation and/or heating from the upward migration of volcanic material. Finally, the anomalous thickness of the crust itself could potentially contribute to lower values of Lg Q .

The Tibetan Plateau is highly fractured due to the suture zones bounding the numerous terranes that make up the plateau and the abundant normal and strike-slip faults in the uppermost 20 km along which the crust is actively deforming (Randall *et al.*, 1995). Since we cannot distinguish between scattering and intrinsic Q , apparent Q can decrease by scattering along the faults and cracks or due to decreased intrinsic Q from internal friction and interstitial fluids in the cracks.

We do not yet have a good understanding of the thermal properties of the Tibetan Plateau; however, the north-central plateau has a number of seismic observations that have been interpreted as evidence for high temperatures in the upper mantle. For example, previous studies, focusing on the northern Tibetan Plateau, have reported observations of large teleseismic S - P travel-time residuals (Molnar and Chen, 1984; Molnar, 1990), slow Rayleigh phase velocities (Brandon and Romanowicz, 1986), low Pn velocities (Zhao and Xie, 1993; McNamara *et al.*, 1995), the absence of Sn propagation (Ni and Barazangi, 1983; McNamara *et al.*, 1995), and large values of shear-wave splitting (McNamara *et al.*, 1994). All of these observations are consistent with anomalously high heat production beneath the northern portion of the plateau. Also, recent volcanic flows of both basaltic and granitic composition are observed at the surface throughout the northern portion of the plateau (Dewey *et al.*, 1988). This would indicate a mantle source of volcanism causing crustal heating as it propagates toward the surface. Crustal heating is likely to significantly increase crustal attenuation (Frankel *et al.*, 1990).

Finally, it may be possible that Lg apparent attenuation is high due to the unusually thick crust itself. The Tibetan Plateau crustal thickness is twice the continental average (Christensen and Mooney, 1995; Molnar, 1988). If Lg is a combination of multiple reflected crustal shear energy, a significantly thicker crustal wave guide will increase the total path length of travel for the multiple reflected waves that make up Lg energy. We analyzed the effect of crustal thickness on apparent Q by computing Lg reflectivity synthetics for several 1D crustal models that varied only in thickness of the crustal wave guide. In the 2- to 4-Hz band, we observed a decrease in Q of about 10% for every 10 km of increased crustal thickness. In general, we did not generate realistic Lg synthetic seismograms or Q values that match the models intrinsic Q input. This is a limitation of a 1D modeling approach that cannot incorporate realistic scattering and may not reflect the actual decay of Lg amplitudes. At this point, however, we will use the 1D results and attempt to correct Lg Q for the increased path lengths in a thickened crust (e.g., Campillo *et al.*, 1985). We can apply a simple correction to our measured Q for the anomalous

crustal thickness of the plateau (70 km) that will allow a more significant comparison with more typical continental regions. Assuming a global average crustal thickness of 40 km, the crustal thickness correction increases our measured Q_0 to be about 470. Since this is still significantly lower than typical observations from stable continental regions, the intrinsic attenuation of the Tibetan Plateau is indicative of a tectonically active region. To further test this idea, more realistic modeling attempts should be made with 2D and 3D synthetic codes that incorporate realistic scattering. Since we are unable to distinguish between the mechanisms discussed, it is likely that any one of these or all in combination may cause a significant enough change in the crustal wave guide to contribute a weakening effect to the amplitude of Lg .

Figure 9 is a plot of Lg apparent $Q(f)$ functions obtained from a variety of sources as well as our results obtained for the Tibetan Plateau. Most results are obtained by the analysis of Lg coda rather than Lg itself. Using Figure 9, it is possible to compare our value of Lg $Q(f)$ for the Tibetan Plateau with other tectonic regions around the world as well as with previously determined values within the Tibetan Plateau. The highest values of Q_0 are for relatively stable continental paths with various frequency power-law values, η (see ECAN, Fig. 9). Low Q and high η values are generally observed in tectonically active regions (see BRP, Fig. 9).

Using a technique similar to ours, Shih *et al.* (1994) reported a Q_0 value, for the Tibetan Plateau, higher than ours with a similar frequency dependence (TIB, Fig. 9). The difference between Shih *et al.* (1994) and this study is likely due to differences in the respective data sets. Shih *et al.* (1994) examined energy in the 2.9- to 3.6-km/sec group velocity window with a much longer period (1 to 6 sec) than that used in this study. Also, many paths used in their study crossed the margins of the plateau. Finally, the CDSN station in Lhasa (LSA) was the only station Shih *et al.* (1994) used within the Tibetan Plateau. Consequently, event-to-station paths do not entirely coincide with the area covered by our study. Our study is an analysis of high-frequency Lg (0.5 to 16 Hz) within the eastern portion of the plateau.

Direct comparison of our results to regions in North America show that Lg Q_0 within the Tibetan Plateau is well below stable continental regions, such as northeastern and central United States, eastern Canada, and Siberia (Fig. 9). Also, the frequency dependence, η , is lower and more similar to the frequency dependence of tectonically active regions, such as the basin and range (Fig. 9). This suggests that the Tibetan Plateau is more similar to a tectonically active region than a stable continental interior or passive margin.

The crust within the Tibetan Plateau is twice as thick as the continental average, and because of this, Lg $Q(f)$ comparisons, with different regions, should be made with caution. Previous authors have shown that earthquakes generally have lower Lg $Q(f)$ than explosions (Chavez and Priestley, 1986). This effect has been attributed to the depth of the event itself. Raytracing indicates that near-surface events (including explosions and shallow earthquakes) gen-

erate L_g energy that propagates within a thin, surface wave guide, while deeper earthquakes (>10 km) propagate L_g throughout the entire crustal wave guide (Campillo *et al.*, 1985). If wave-guide thickness effects $L_g Q$, then the low $L_g Q$ of the Tibetan Plateau may be a function of the doubly thick crust (~ 70 km) and may not uniquely reflect the actual rock properties (i.e., intrinsic Q). For $L_g Q$ comparisons between regions of varying crustal thicknesses, values of Q may need to be corrected for wave-guide thickness.

Xie and Mitchell (1991) obtained a tomographic map of the laterally varying L_g coda Q in southern Eurasia. They predict a Q_0 that increases from the south to the north from about 250 to 350 across the Tibetan Plateau. These $L_g Q_0$ values can have errors that range from about 10% to 15% (Xie, 1993). Taking into account uncertainties in the measurement procedures and assuming a close resemblance between L_g coda Q and $L_g Q$, we find that our average Q_0 of 366 ± 37 is in close agreement with the results ($Q_0 \sim 350$) obtained by Xie and Mitchell (1991) for the Tibetan Plateau. If we assume that our signal-to-noise criteria was successful at reducing random error from the amplitude observations, then our resultant error bars are likely to be a measure of the lateral heterogeneity of the attenuation structure within the Tibetan Plateau. Based on our qualitative analysis of L_g amplitudes that propagate within the plateau, we were unable to detect lateral variations. However, the roughly 10% uncertainty in our average $L_g Q_0$ indicates that such heterogeneities could exist.

The inverse method used in our analysis utilizes many source-receiver paths, so it consequently solves for an average regional $L_g Q$ estimate. It is likely that individual paths, or else regionalized sets of paths, should be analyzed to potentially correlate variable $L_g Q$ with regional structures across the plateau. Xie (1993) has developed a method in which both L_g source spectra and path-dependent Q can be estimated simultaneously. The technique was demonstrated to be successful using one explosion recorded at several stations in central Asia. The most significant advantage of Xie's technique is that it allows values of Q_0 and η to be variable among paths (see SIB and CAS, Fig. 9). Such information would be useful in explaining the uncertainties in our $Q(f)$ results; however, when applied to earthquake sources, the radiation pattern may be more significant than when using explosion sources. Consequently, with few observations, interpretation of path-dependent $L_g Q$ might prove difficult. Future analysis of $L_g Q$ within the Tibetan Plateau will test the applicability of path-variable $L_g Q$ to better explain our uncertainties with laterally heterogeneous attenuation structure within the Tibetan Plateau.

Implications for Event Discrimination. We can qualitatively demonstrate the significance of an accurate knowledge of regional attenuation in event discrimination efforts. Specifically, the northern boundary of the plateau effectively eliminates the ability to discriminate between naturally occurring earthquakes and nuclear explosions with the use of

P/L_g ratios (e.g., Walter *et al.*, 1995). For example, Figure 10 shows broadband seismograms at two separate stations from an earthquake (91.257.13.17.47) and a nuclear explosion (92.142.05.00.01) at similar distances (998 and 793 km, respectively) to the north of our array (see Fig. 2). At station TUNL, north of the northern margin of the plateau, a clear distinction can be seen in the relative amplitudes of the P and L_g phases. L_g energy for the earthquake is significantly greater, relative to the first arrivals, than for the explosion. This suggests that at TUNL, the P/L_g ratio would be an effective discriminant. However, for stations within the plateau (e.g., ERDO, Fig. 10), L_g paths from the two events cross the northern boundary of the plateau, and L_g energy is significantly reduced for both events relative to P -wave energy. In this case, P/L_g ratios are similar for these two events, and a distinction cannot easily be made between the earthquake and the nuclear explosion using P/L_g ratios. These observations demonstrate that if restricted to analysis of event paths that cross the boundaries of the Tibetan Plateau, discrimination and yield estimation efforts, based on L_g , will be erroneous. Either additional methods or a more accurate understanding of regional variations in attenuation is required for the Tibetan Plateau.

Conclusions

Our data set represents the first observations of L_g arrivals for source-receiver paths confined entirely to the Tibetan Plateau. From our qualitative analysis of L_g amplitudes, we conclude that L_g is generated and does propagate within the Tibetan Plateau. However, attenuation is high, and L_g is not observed for paths greater than about 600 to 700 km for our data set. We find an $L_g Q$ value that is similar to values determined for the tectonically active basin and range of North America and that is significantly less than $L_g Q$ determined for typical continental interior and passive margin regions. Previous studies, which relied on distant stations, observed that L_g does not propagate through the southern boundary of the Tibetan Plateau. We have shown that both the northern and southern boundaries of the plateau cause inefficient L_g transmission. Both the Himalayan boundary thrust to the south and the Kunlun front to the north are barriers to L_g propagation due to either scattering along fractures or simply due to the change in crustal thickness across the margin. An accurate understanding of regional variations in attenuation is critical to current efforts to discriminate between earthquakes and explosions in Asia. The attenuation within the Tibetan Plateau and the blockage of L_g transmission at its margins have clear implications for many common nuclear monitoring discriminants, such as P/L_g and P/S_n ratios. Since L_g will be greatly attenuated for any path crossing the boundaries of the plateau and since attenuation is high within the plateau for both L_g and S_n , other techniques are required for event discrimination in this region.

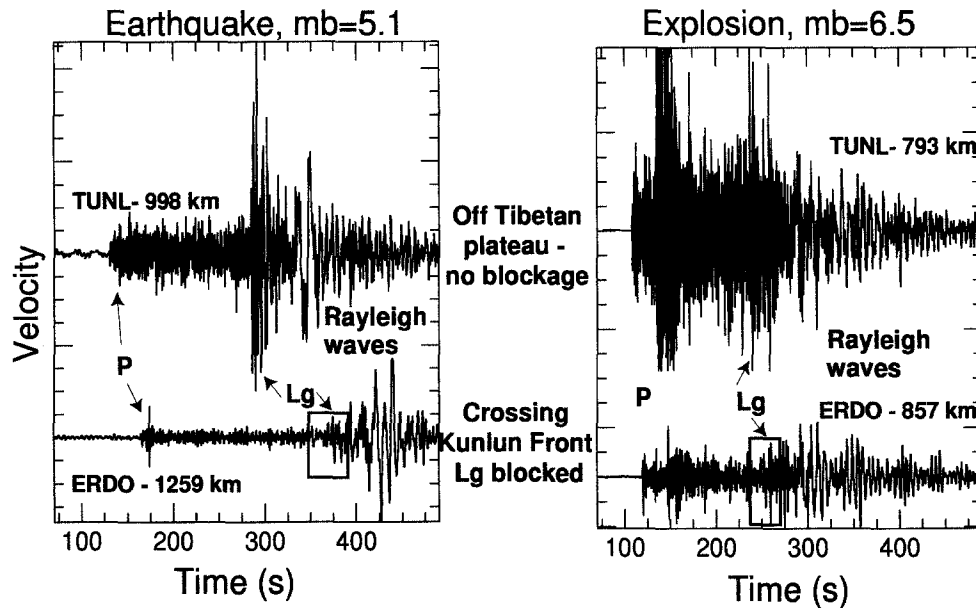


Figure 10. Broadband vertical-component seismograms demonstrate the ineffectiveness of P/Lg ratios for event discrimination using paths crossing the northern boundary of the Tibetan Plateau. Seismograms are shown for two stations. One outside of the plateau, TUNL, and one within the plateau, ERDO, illustrating Lg blockage. Note the much larger P/Lg value for the explosion than for the earthquake at TUNL. At ERDO, the P/Lg ratios are comparable. The Lg group velocity (3.6 to 3.1 km/sec) is shown within the box. Note the azimuths from the earthquake to stations TUNL and ERDO differ by only a few degrees, suggesting that the effect is not due to radiation pattern of the source. Epicentral distances are shown next to each trace. (a) Earthquake from northeast of the plateau (91.257.13.15.47, $mb = 5.1$). (b) Underground nuclear explosion from north of the Tibetan Plateau at the Chinese Lop Nor test site (92.142.05.00.01, $mb = 6.5$). Explosion P waves at TUNL are clipped.

Acknowledgments

The authors would like to thank the many scientists and field workers who endured the hardships of the Tibetan Plateau and greatly contributed to the success of this experiment. We would especially like to thank F. Wu and R. Zeng whose persistence made this cooperative effort possible. Contributors included Chinese participants from the Institute of Geophysics, State Seismological Bureau, PRC, and the Seismological Bureaus of the Qinghai Province and the Tibetan Autonomous Region. The U.S. participants in the field program included F. Wu (SUNY-Binghamton), R. Busby (PIC-LDGO), R. Kuehnel (Carnegie-DTM), G. Randall, G. Wagner, S. Owens, and M. Salvador (USC). This project was supported by NSF Grants EAR-9004428, EAR-9196115, and EAR-9206815 and by AFOSR Contract F49620-94-1-0066DEF to USC. $Q(f)$ inversion work was supported by LLNL in the summer of 1994 and performed under the auspices of the U.S. Department of Energy by Lawrence Livermore National Laboratory under Contract W-7405-ENG-48. H. Benz wrote the original inversion computer code and supplied valuable advice on Lg propagation. G. Pavlis was instrumental in noting the importance of these observations early on. Maps were created using GMT (Wessel and Smith, 1991).

References

- Aki, K. (1980a). Scattering and attenuation of shear waves in the lithosphere. *J. Geophys. Res.* **85**, 6496–6504.
- Aki, K. (1980b). Scattering and attenuation of shear waves in the lithosphere from 0.05 to 25 Hz. *Phys. Earth Planet. Interiors* **21**, 50–60.
- Atkinson, G. M. and R. F. Merez (1992). The shape of ground motion attenuation curves in southeastern Canada. *Bull. Seism. Soc. Am.* **82**, 2014–2031.
- Banda, E., L. W. Deichmann, L. W. Braille, and J. Ansgore (1982). Amplitude study of the Pg phase. *J. Geophys.* **51**, 153–164.
- Bath, M. (1954). The elastic waves of Lg and Rg along Euroasiatic paths. *Ark. Geophys.* **2**, 295–342.
- Benz, H. M., R. Buland, and A. Frankel (1994). Source and structure studies using the U.S. national seismographic network (abstract). *Sixth Annual IRIS Workshop*, 7.
- Bouchon, M. (1982). The complete synthesis of seismic crustal phases at regional distances. *J. Geophys. Res.* **87**, 1735–1741.
- Brandon, C. and A. Romanowicz (1986). A “NO-LID” zone in the central Chang-Thang platform of Tibet: evidence from pure path phase velocity measurements of long-period Rayleigh waves. *J. Geophys. Res.* **91**, 6547–6564.
- Burger, R. W., P. G. Somerville, L. S. Barker, R. B. Herrmann, and D. V. Helmberger (1987). The effect of crustal structure on strong ground motion attenuation relations in eastern North America. *Bull. Seism. Soc. Am.* **77**, 120–139.
- Cao, S. and K. J. Muirhead (1993). Finite difference modeling of Lg blockage. *Geophys. J. Int.* **115**, 85–96.
- Campillo, M., M. Bouchon, and B. Massinon (1984). Theoretical study of the excitation, spectral characteristics, and geometrical attenuation of regional seismic phases. *Bull. Seism. Soc. Am.* **74**, 1395–1411.
- Campillo, M. (1990). Propagation and attenuation characteristics of the crustal phase Lg . *Pageoph* **132**, 1–17.
- Campillo, M. (1987). Lg wave propagation in a laterally varying crust and the distribution of the apparent quality factor in central France. *J. Geophys. Res.* **92**, 12604–12614.

- Campillo, M., J. Plantet, and M. Bouchon (1985). Frequency-dependent attenuation in the crust beneath central France from Lg waves: data analysis and numerical modeling, *Bull. Seism. Soc. Am.* **75**, 1395–1411.
- Chavez, D. E. and K. F. Priestley (1986). Measurement of frequency dependent Lg attenuation in the Great Basin, *Geophys. Res. Lett.* **13**, 551–554.
- Christensen, N. I. and W. D. Mooney (1995). Seismic velocity structure and composition of the continental crust: a global view, *J. Geophys. Res.* **100**, 9761–9788.
- Dewey, J. F., R. M. Shackleton, F. R. S. Chang Cheng, and S. Yiyin (1988). The tectonic evolution of the Tibetan Plateau, *Phil. Trans. Roy. Soc. London* **327**, 379–413.
- Ewing, W. M., W. S. Jardetzky, and F. Press (1957). *Elastic Waves in Layered Media*, McGraw-Hill, New York, 380 pp.
- Frankel, A., A. McGarr, J. Bicknell, J. Mori, L. Seeber, and E. Cranswick (1990). Attenuation of high-frequency shear waves in the crust: measurements from New York state, South Africa, and southern California, *J. Geophys. Res.* **95**, 17441–17457.
- Gregersen, S. (1984). Lg-wave propagation and crustal structure differences near Denmark and the North Sea, *Geophys. J. R. Astr. Soc.* **79**, 217–234.
- Gutenberg, B. (1955). Channel waves in the Earth's crust, *Geophysics* **20**, 283–294.
- Herrmann, R. B. and J. Kijko (1983). Modeling some empirical vertical component Lg relations, *Bull. Seism. Soc. Am.* **73**, 161–181.
- Herrin, E. and J. Richmond (1960). On the propagation of the Lg Phase, *Bull. Seism. Soc. Am.* **50**, 197–210.
- Kennett, B. L. (1986). Lg waves and structural boundaries, *Bull. Seism. Soc. Am.* **76**, 1133–1141.
- Kennett, B. L. N., S. Gregerson, S. Mykkeltveit, and R. Newmark (1985). Mapping of crustal heterogeneity in the North Sea via the propagation of Lg-phases, *Geophys. J. R. Astr. Soc.* **83**, 299–306.
- Knopoff, L., F. Schwab, and E. Kausel (1973). Interpretation of Lg, *Geophys. J. R. Astr. Soc.* **33**, 389–404.
- McNamara, D. E., T. J. Owens, P. G. Silver, and F. T. Wu (1994). Shear wave anisotropy beneath the Tibetan Plateau, *J. Geophys. Res.* **99**, 13655–13665.
- McNamara, D. E., T. J. Owens, and W. R. Walter (1995). Observations of regional phase propagation across the Tibetan Plateau, *J. Geophys. Res.* **100**, 22215–22229.
- Menke, W. (1990). *Geophysical Data Analysis: Discrete Inverse Theory*, Academic Press, Inc., San Diego, California.
- Mitchell, B. J. (1975). Regional Rayleigh wave attenuation in North America, *J. Geophys. Res.* **80**, 4904–4916.
- Mitchell, B. J. (1981). Regional variation and frequency dependence of Q_β in the crust of the United States, *Bull. Seism. Soc. Am.* **71**, 1531–1538.
- Mitchell, B. J. (1995). Anelastic structure and evolution of the continental crust and upper mantle from seismic surface wave attenuation, *Rev. Geophys.* **33**, 441–462.
- Molnar, P. and J. Oliver (1969). Lateral variations of attenuation in the mantle and discontinuities in the lithosphere, *J. Geophys. Res.* **74**, 2648–2682.
- Molnar, P. and W. P. Chen (1984). S-P travel time residuals and lateral inhomogeneity in the mantle beneath Tibet and the Himalaya, *J. Geophys. Res.* **89**, 6911–6917.
- Molnar, P. (1988). A review of geophysical constraints on the deep structure of the Tibetan Plateau, the Himalaya and the Karakoram, and their tectonic implications, *Trans. Roy. Soc. London A* **327**, 33–88.
- Molnar, P. (1990). S-wave residuals from earthquakes in the Tibetan region and lateral variations in the upper mantle, *Earth Planet. Sci. Lett.* **101**, 68–77.
- Ni, J. and M. Barazangi (1983). High frequency seismic wave propagation beneath the Indian shield, Himalayan arc, Tibetan Plateau and surrounding regions: high uppermost mantle velocities and efficient propagation beneath Tibet, *Geophys. J. R. Astr. Soc.* **72**, 665–689.
- Nuttli, O. W. (1973). Seismic wave attenuation and magnitude relations for eastern North America, *J. Geophys. Res.* **78**, 876–885.
- Nuttli, O. W., G. A. Bollinger, and D. W. Griffiths (1979). On the relation between modified mercalli intensity and body wave magnitude, *Bull. Seism. Soc. Am.* **69**, 893–910.
- Oliver, J. and M. Ewing (1957). Higher mode surface waves and their bearing on the structure of the Earth's mantle, *Bull. Seism. Soc. Am.* **47**, 187–204.
- Owens, T. J., G. E. Randall, F. T. Wu, and R. S. Zeng (1993a). PASSCAL instrument performance during the Tibetan Plateau passive seismic experiment, *Bull. Seism. Soc. Am.* **83**, 1959–1970.
- Owens, T. J., G. E. Randall, D. E. McNamara, and F. T. Wu (1993b). Data Report for the 1991–92 Tibetan Plateau passive-source seismic experiment, PASSCAL Data Rep. #93-005.
- Pec, K. (1962). Continental waves in central Europe, *Pr. Geophys. Ustern Cesk. Acad. Ved.* **102**, 123–193.
- Press, F. and M. Ewing (1952). Two slow surface waves across North America, *Bull. Seism. Soc. Am.* **42**, 219–228.
- Randall, G. E., C. J. Ammon, and T. J. Owens (1995). Moment-tensor estimation using regional seismograms from portable network deployments, *Geophys. Res. Lett.* **22**, 1665–1668.
- Richter, C. F. (1958). *Elementary Seismology*, W. H. Freeman, New York.
- Rodgers, A. J., J. F. Ni, and T. M. Hearn (1995). Pn, Sn, and Lg propagation in the Middle East, *Bull. Seism. Soc. Am.* (submitted for review).
- Ruzaikin, A., I. Nersesov, V. Khalturin, and P. Molnar (1977). Propagation of Lg and lateral variations in crustal structure in Asia, *J. Geophys. Res.* **82**, 307–316.
- Saha, B. P. (1961). The seismic Lg waves and their propagation along the granite layer of the crust of Indian sub-continent, *Indian J. Meteorol. Geophys.* **12**, 609–618.
- Sereno, T. J. (1990). Frequency-dependent attenuation in eastern Kazakhstan and implications for seismic detection thresholds in the Soviet Union, *Bull. Seism. Soc. Am.* **80**, 2089–2105.
- Sereno, T. J., S. R. Bratt, and T. C. Bache (1988). Simultaneous inversion of regional wave spectra for attenuation and seismic moment in Scandinavia, *J. Geophys. Res.* **93**, 2019–2035.
- Shih, X. R., K. Y. Chun, and T. Zhu (1994). Attenuation of 1–6 s Lg waves in Eurasia, *J. Geophys. Res.* **99**, 23859–23874.
- Street, R. L., R. B. Herrmann, and O. W. Nuttli (1975). Spectral characteristics of the Lg wave generated by central United States earthquakes, *Geophys. J. R. Astr. Soc.* **41**, 51–63.
- Walter, W. R., K. M. Mayeda, and H. J. Patton (1995). Phase and spectral ratio discrimination between NTS earthquakes and explosions. Part I: Empirical observations, *Bull. Seism. Soc. Am.* **85**, 1050–1067.
- Wessel, P. and W. Smith (1991). Free software helps display data, *EOS* **72**, 445–446.
- Xie, J. and B. J. Mitchell (1991). Lg coda Q across Eurasia, *Yield and Discrimination Studies in Stable Continental Regions*, 77–91.
- Xie, J. (1993). Simultaneous inversion for source spectrum and path Q using Lg with application to three Semipalatinsk explosions, *Bull. Seism. Soc. Am.* **83**, 1547–1562.
- Zhao, L. S. and J. Xie (1993). Lateral variations in compressional velocities beneath the Tibetan Plateau from Pn traveltimes tomography, *Geophys. J. Int.* **115**, 1070–1084.

Department of Geological Sciences
University of South Carolina
Columbia, South Carolina 29208
(D.E.M., T.J.O.)

Earth Sciences Division
Lawrence Livermore National Laboratory
Livermore, California 94550
(W.R.W.)